Electronic Supplementary Material (ESI) for Journal of Materials Chemistry A.

Supporting information

Step-wise Controlled Growth of Metal@TiO_2 Core-shell with Plasmonic Hot Spots and Their Photocatalytic Properties

Teera Butburee,[a] *Yang Bai,*[a] *Jian Pana*[a,b] *Xu Zong,*[a] *Chenghua Sun,*[c] *Gang Liu,*[b] *and Lianzhou Wang**[a]

[a]Nanomaterials Centre, School of Chemical Engineering and Australian Institute for Bioengineering and Nanotechnology, the University of Queensland, St Lucia, QLD, 4072, Australia, *Email: l.wang@uq.edu.au

[b]Shenyang National Laboratory for Materials Science, Institute of Metal Research, Chinese Academy of Sciences, 72 Wenhua RD, Shenyang 110016, China. *Email: gangliu@imr.ac.cn

[c]School of Chemistry, Monash University, Clayton, VIC 3800, Australia.

Keywords: plasmonic metals, TiO_2, core-shells, morphological control, photocatalysis

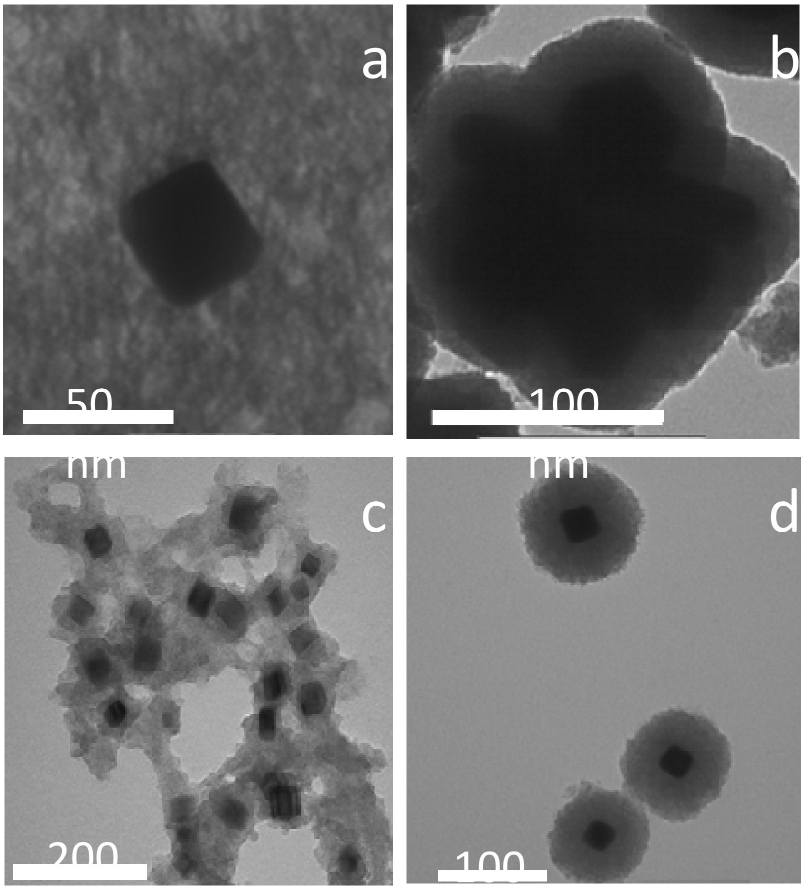

Figure S1. a) TEM image of a metal core after the shell coating procedure, herein the metal cores were surface modified only with surfactant CTAB, but without MCA surface modification. It is clear that TiO_2 cannot deposit on the metal surface because of the long aliphatic cationic CTAB capping agent. **b)** a TEM image of core-shell aggregates for the samples subject to the removal of all surfactants by Piranha reagent (3:1 of $NH_4OH:H_2O_2$). In this case, although TiO_2 can be deposited on the surface but the metal cores suffer from aggregation; the morphology of core-shell structure is difficult to control. **c)** TEM image of the core-shell structure obtained by fast hydrolysis of $TiCl_3$ precursor under high pH conditions. Because of the rapid formation of TiO_2 nuclei it is difficult to control the morphology of particles. **d**) TEM image of the core-shell structures under appropriate condition.

Time dependent-TiO_2 shell thickness observation: In this part, we controlled the thickness of TiO_2 shell by the reaction time. First, the pH of both Au-core solution and 10 mL of 1 M $TiCl_3$ precursor were adjusted to 2.25 in a similar way as Pd@TiO_2. The 50 mM $TiCl_3$ precursor was then added to the Au core solution under vigorous stirring. Monitored by pH meter, the pH of the reaction was kept at 2.25±0.05 throughout the reaction by dropping 1M NH_4OH when the pH decreased. 2 mL of the solution was pipetted from the reaction (at10, 20, 30, 40, 50 and 60 minutes), and centrifuged immediately to stop the reaction. The top aliquot was poured to remove the exceed $TiCl_3$ precursor. We investigated time-dependent thickness growth of TiO_2 shell by TEM.

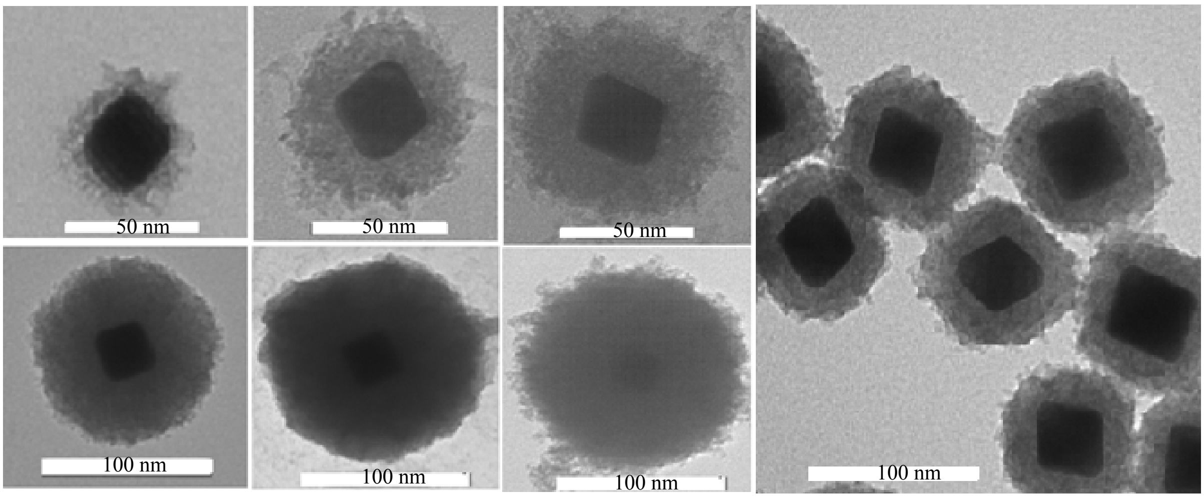

Figure S2. TEM Images of time-dependent TiO_2 shell thickness growth of octahedral Au@TiO_2 when the reaction time was 10, 20, 30, 40, 50 and 60 minutes **(a-f)** respectively. **g)** TEM image indicating the uniformity of the particle distribution.

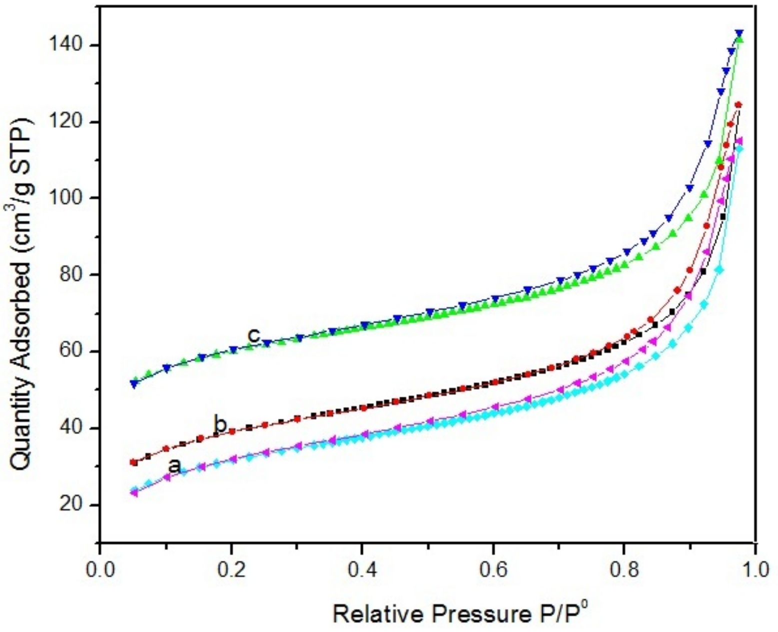

Figure S3. N_2 adsorption-desorption isotherms of the Pd@TiO_2 after calcinations of samples with a) 25, b) 50 and c) 75 nm TiO_2 thick shell at 450 °C respectively.

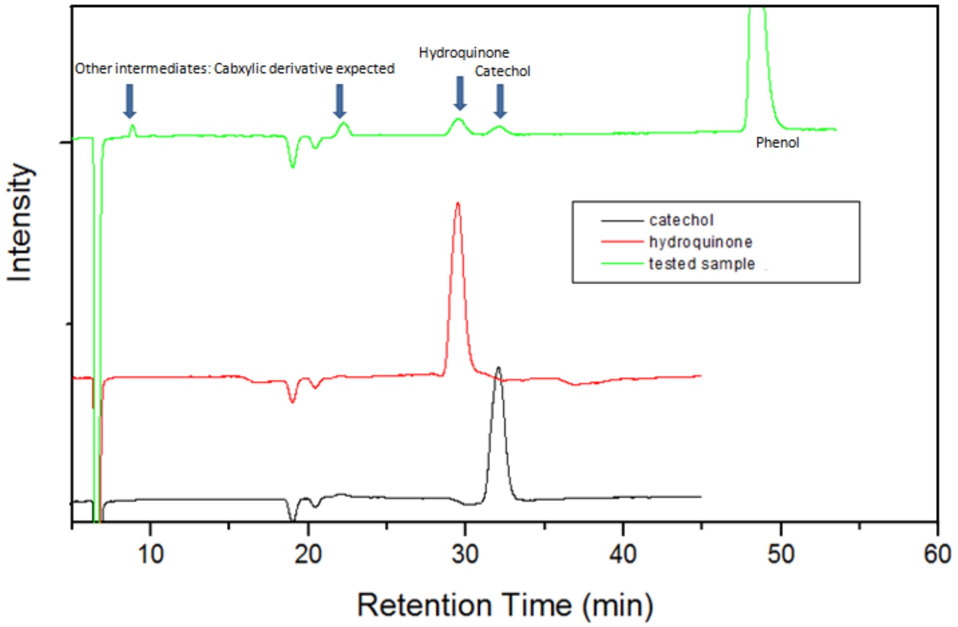

Figure S4. Qualitative analysis of the intermediate of the reaction between phenol and Pd@TiO$_2$. Hydroquinone and catechol are present after few minutes of reaction, suggesting that the degradation process could pass through hydroxylation process by ·OH radicals before breaking the ring to the smaller molecules such as carboxylic derivatives.

HPLC analysis was performed by Shimadzu Prominence HPLC. The column was Biorad Aminex HPX-87X (7.8x300 mm) at 50 °C. 5 mM H_2SO_4 was used as the mobile phase with the flow rate of o.6 mL/min. The detector was RID-10.

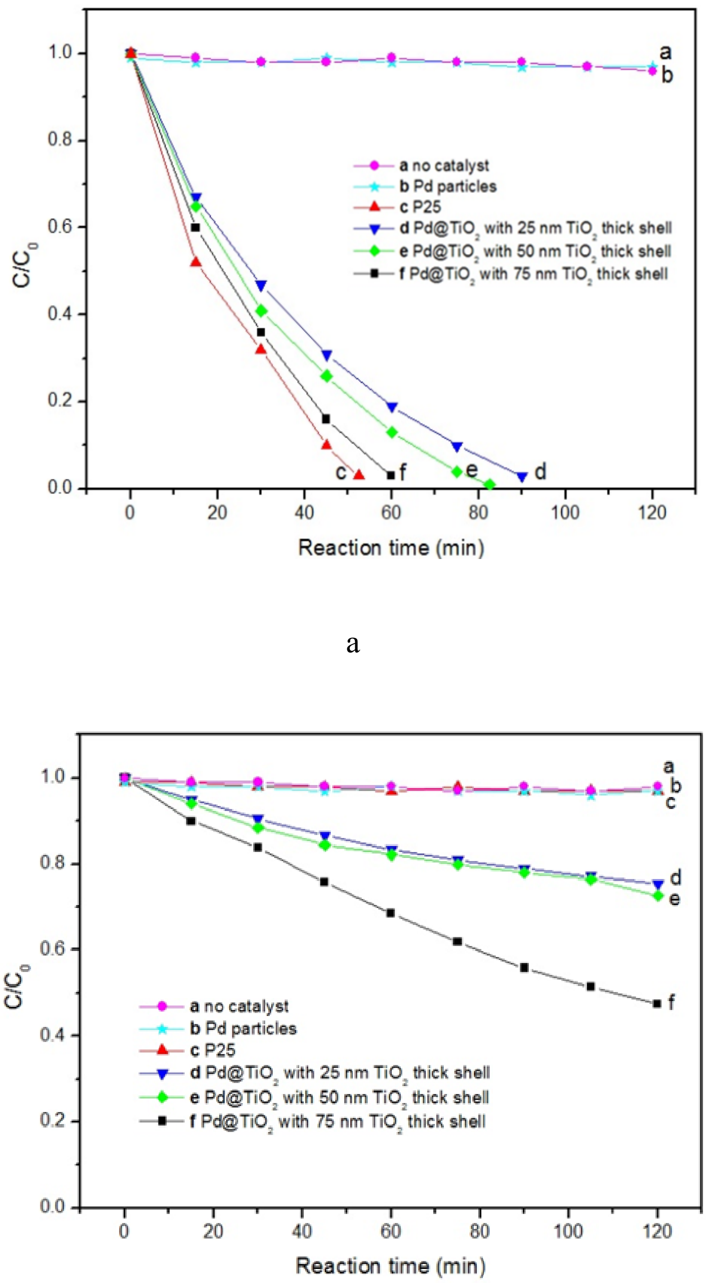

a

b

Figure S5. Photocatalytic phenol degradation of samples a) under solar simulator (AM 1.5), and b) under light with wavelength > 495 nm (solar simulator with 495 nm cut-off filter).

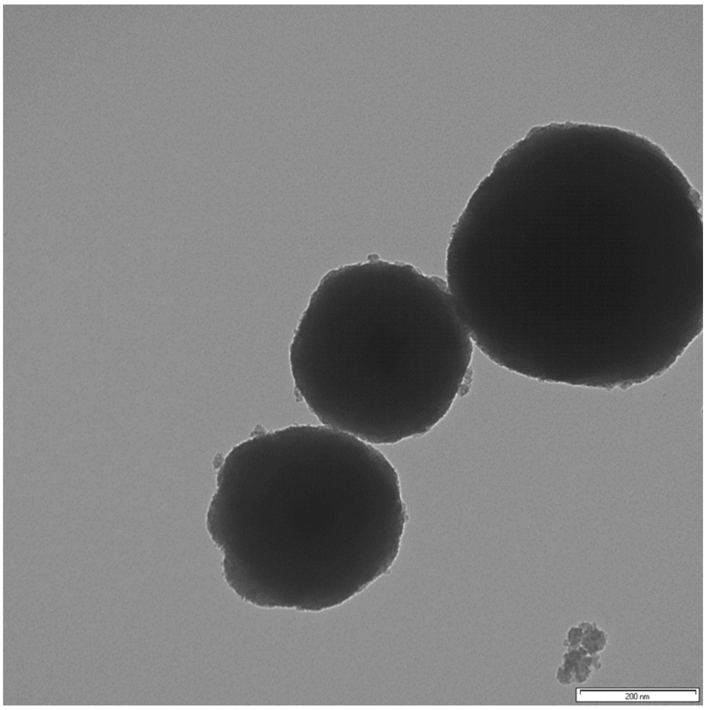

Figure S6. TEM image of Pd@TiO_2 core-shell sample with thicker shells of >75 nm. Due to the large shell thickness, it's difficult to distinguish the metal core from TiO_2 shells and the particle morphology become less uniform.